

GlcNAc 2-epimerase Can Serve a Catabolic Role in Sialic Acid Metabolism

Sarah J. Luchansky¹, Kevin J. Yarema², Saori Takahashi³, and Carolyn R. Bertozzi^{1, 4-6}

Departments of ¹Chemistry and ⁴Molecular and Cell Biology and ⁵Howard Hughes Medical Institute, University of California and ⁶Center for Advanced Materials, Materials Science Division, Lawrence Berkeley National Laboratory, Berkeley, CA, 94720

²Current address: Whitaker Biomedical Engineering Institute, The Johns Hopkins University, Baltimore, MD, 21218

³Department of Bioengineering, Akita Research Institute of Food and Brewing, 4-26, Sanuki, Arayamachi, Akita 010-1623 Japan

Address correspondence to: Carolyn R. Bertozzi

Phone: (510) 643-1682

Fax: (510) 643-2628

Email: bertozzi@cchem.berkeley.edu

Running title: Role of GlcNAc 2-epimerase

SUMMARY

Sialic acid is a major determinant of carbohydrate-receptor interactions in many systems pertinent to human health and disease. *N*-Acetylmannosamine (ManNAc¹) is the first committed intermediate in the sialic acid biosynthetic pathway, thus the mechanisms that control intracellular ManNAc levels are important regulators of sialic acid production. UDP-*N*-Acetylglucosamine (UDP-GlcNAc) 2-epimerase and GlcNAc 2-epimerase are two enzymes capable of generating ManNAc from UDP-GlcNAc and GlcNAc, respectively. While the former enzyme has been shown to direct metabolic flux toward sialic acid *in vivo*, the function of the latter enzyme is unclear. Here we study the effects of GlcNAc 2-epimerase expression on sialic acid production in cells. A key tool we developed for this study is a cell-permeable, small molecule inhibitor of GlcNAc 2-epimerase designed based on mechanistic principles. Our results indicate that, unlike UDP-GlcNAc 2-epimerase which promotes biosynthesis of sialic acid, GlcNAc 2-epimerase can serve a catabolic role, diverting metabolic flux away from the sialic acid pathway.

INTRODUCTION

Carbohydrate-receptor interactions participate in numerous cell-cell recognition events in eukaryotes (1-4). Of the nine monosaccharides that constitute mammalian polysaccharides, the common terminal residue sialic acid stands out as a major determinant of cell-cell interactions. Sialic acid is a component of sialyl Lewis x (sLe^x), a tetrasaccharide that binds the selectin family of adhesion molecules and initiates inflammatory leukocyte adhesion (5). Sialic acid is also the major binding determinant of Siglecs, a family of sialic acid-binding lectins that are involved in many processes including B-cell signaling and activation (6).

Because of the prominent role of sialic acid in cell surface recognition, there is considerable interest in the regulatory mechanisms that control its biosynthesis and presentation on the cell surface (Figure 1) (7). The first committed intermediate in the biosynthesis of sialic acid is *N*-acetylmannosamine (ManNAc), which is phosphorylated by ManNAc 6-kinase (8,9) to initiate sialic acid biosynthesis in the cytosol. The subsequent action of sialic acid synthase (10), followed by an unknown phosphatase, yields sialic acid, which is then transformed into CMP-sialic acid by CMP-sialic acid synthetase in the nucleus (11,12). After transport into the Golgi compartment, the sialyltransferases utilize this substrate to sialylate the terminal position of oligosaccharide chains. Transcriptional regulation of sialyltransferases is one mechanism for controlling the production of certain sialylated epitopes such as polysialic acid (13), sLe^x (5) or α -2,6-linked sialyllactosamine (6).

The overall production of sialic acid in mammalian cells appears to be regulated by the availability of ManNAc which, in principle, can be synthesized through two possible routes. UDP-*N*-Acetylglucosamine (UDP-GlcNAc) 2-epimerase (Figure 1) catalyzes the conversion of UDP-GlcNAc to ManNAc and has been implicated as a major source of ManNAc in mammalian cells (14-16). High levels of CMP-sialic acid inhibit UDP-GlcNAc 2-epimerase, thereby reducing flux in the sialic acid biosynthetic pathway (17). A second enzyme, GlcNAc 2-epimerase, can also produce ManNAc by catalyzing the reversible epimerization of GlcNAc to

ManNAc (18-20). However, GlcNAc is thermodynamically favored with an equilibrium ratio of 3.9:1 (21). Thus, it is possible that GlcNAc 2-epimerase functions to divert ManNAc away from sialic acid biosynthesis and into other glycosylation or glycolytic pathways. Additionally, human GlcNAc 2-epimerase binds the protease renin (22), but as of yet no functional significance for this interaction has been demonstrated (23). In summary, the role of UDP-GlcNAc 2-epimerase in the biosynthesis of sialic acid has been clearly established, but the cellular role of GlcNAc 2-epimerase remains unclear.

Northern analysis of the mRNAs encoding these epimerases has revealed some differences in their tissue distribution in mice. UDP-GlcNAc 2-epimerase is highly expressed in the liver (9,24), while GlcNAc 2-epimerase is highly expressed in the kidney (23). The enzymes do appear to have some overlapping tissue distribution, however, suggesting either that one enzyme is redundant or the functions they perform are distinct.

To investigate the function of GlcNAc 2-epimerase in cells, we identified a cell line lacking the enzyme, introduced the gene into these cells and studied the effects of GlcNAc 2-epimerase expression on sialic acid biosynthetic flux. We found that GlcNAc 2-epimerase expression suppressed sialic acid production in response to exogenous addition of ManNAc or ManNAc analogs. Furthermore, guided by a proposed chemical mechanism (21), we prepared two novel substrate-based inhibitors of GlcNAc 2-epimerase and demonstrated that one of these inhibitors functions within cells to block the action of the enzyme. Using the inhibitor as a tool, we confirmed that the phenotype resulting from GlcNAc 2-epimerase expression was indeed due to direct action of the enzyme. Based on these data, we propose that GlcNAc 2-epimerase plays a catabolic role in sialic acid metabolism.

EXPERIMENTAL PROCEDURES

Materials

Pfu DNA polymerase was from Stratagene. All PCR reactions were performed on an MJ Research DNA Engine. The vector pDsred2-N1 was from Clontech. His-bind resin and pET28b(+) were from Novagen. All restriction enzymes and T4 DNA ligase were from New England Biolabs. DNA sequencing was performed by the UC Berkeley DNA Sequencing Facility or Davis Sequencing. RPMI-1640 media, Lipofectamine PLUS, Hygromycin, Zeocin, the Micro-FastTrack 2.0 mRNA Isolation System, the Superscript First-Strand Synthesis System for RT-PCR and the FlpIn system were purchased from Invitrogen Life Technologies. FITC-avidin, penicillin, streptomycin, biotin hydrazide and GlcNAc were purchased from Sigma. ManNAc was purchased from Pfanstiehl. Fetal calf serum (FCS) was from Hyclone. MAA-FITC and LFA-FITC were purchased from EY Laboratories and TML-biotin was from Calbiochem. Cell densities were determined using a Coulter Z2 cell counter. Flow cytometry data were acquired using a Coulter EPICS XL-MCL flow cytometer or a BD Biosciences FACSCalibur flow cytometer equipped with a 488 nm argon laser. For flow cytometry experiments, 10,000 live cells were analyzed and all data points were collected in triplicate.

All chemical reagents were obtained from commercial suppliers and used without further purification unless otherwise noted. All NMR spectra were measured with a Bruker AMX-300, AMX-400 or DRX-500 MHz spectrometer as noted. All coupling constants (*J*) are reported in Hz. Mass spectral data were obtained from the UC Berkeley Mass Spectrometry Laboratory. Reversed-phase HPLC was performed using a Rainin Dynamax SD-200 HPLC system with 220 nm detection on a Microsorb C₁₈ analytical column (4.6 x 250 mm) at a flow rate of 1.0 ml/min or a preparative column (25 x 250 mm) at a flow rate of 20 ml/min. Ac₄ManLev (25), Ac₄ManNAz (26) and compound **2** (27) were synthesized as previously described.

Expression of GlcNAc 2-epimerase in Jurkat cells

For mammalian expression, the GlcNAc 2-epimerase gene was cloned into the pcDNA5/FRT vector, a component of the FlpIn system, by digestion of pUKHRB6 (20) and pcDNA5/FRT with *EcoR* I and subsequent ligation with T4 DNA ligase. The correct product was confirmed by DNA sequencing and the vector was denoted pSJLG2E/FRT. The gene encoding the red fluorescent protein (dsRed) was also cloned into pcDNA5/FRT. The vectors pcDNA5/FRT and pDsRed2-N1 were digested with *Hind* III and *Not* I and the gene encoding dsRed was ligated into pcDNA5/FRT with T4 DNA ligase. The correct product was confirmed by DNA sequencing and the vector was denoted pSJLRFP/FRT.

Jurkat cell lines stably expressing GlcNAc 2-epimerase were generated with the FlpIn system according to the manufacturer's instructions. Briefly, Jurkat cells were transfected with pFRT/*lacZeo* using Lipofectamine PLUS. After selection using Zeocin, stable transfectants were isolated that contain Flp recombinase sites flanking the Zeocin resistance gene. Clonal populations were isolated using "feeder" Jurkat cells as previously described (28) and the gene encoding the red fluorescent protein (dsRed) was introduced into selected clones to determine whether the site of incorporation yielded high, homogeneous gene expression. The vectors pSJLRFP/FRT and pOG44 (encoding the Flp recombinase) were introduced into various Zeocin-resistant clones and cells were selected for Hygromycin resistance. The cells were analyzed by flow cytometry and one Zeocin-resistant cell line was selected as the host for GlcNAc 2-epimerase (denoted wt*). The vectors pSJLG2E/FRT and pOG44 were introduced into wt* cells using Lipofectamine PLUS. After selection in the presence of Hygromycin, the resulting population was denoted G2E*.

Jurkat and Jurkat-derived cell lines were maintained in a 5.0% CO₂, water-saturated atmosphere at 37 °C and grown in RPMI-1640 media supplemented with penicillin (100 units/ml) and streptomycin (0.1 mg/ml). Wt* cells were grown in the presence of Zeocin (100 µg/ml) and G2E* cells were grown in the presence of Hygromycin (300 µg/ml). Typically, both

Role of GlcNAc 2-epimerase

cell lines were grown in T-25 flasks and cell densities were maintained between 2.0×10^5 and 1.6×10^6 cells/ml.

RT-PCR on wt and G2E* cells*

Messenger RNA from 5.0×10^6 of Jurkat, wt* and G2E* cells was isolated using the Micro-FastTrack 2.0 mRNA Isolation kit according to the manufacturer's instructions. cDNA was synthesized using the SuperScript First-Strand Synthesis kit and oligo dT primers. The GlcNAc 2-epimerase gene was amplified using the following primers: forward primer: 5'-GCAGGTATGGATGTATTGTCG-3', reverse primer: 5'-CTGTCACTGTAACCCATGAGG-3' and the β -actin gene was detected with the following primers: forward primer: 5'-GTGGGCCGCTCTAGGCACAA-3', reverse primer: 5'-CTCTTTGATGTCACGCACGATTT C-3'. PCR was performed using *Pfu* DNA polymerase and the following cycling conditions: 96 °C for 3.0 min, then 30 cycles of 96 °C for 45 s, 55 °C for 45 s, 72 °C for 90 s, then 72 °C for 5.0 min.

Flow cytometry

Cells were seeded at a density of 2.0×10^5 cells/ml and incubated for three days with the compounds indicated. Cells were then washed and stained with either biotin hydrazide and FITC-avidin to detect ketones (29), or phosphine-FLAG and anti-FLAG-FITC to detect azides (30). For lectin staining, wt* and G2E* cells were washed twice with wash buffer (PBS, pH 7.1, containing 1.0% FCS) and incubated with TML-biotin for 1.0 h at room temperature. Following incubation, cells were washed three times with wash buffer and stained with FITC-avidin (1:250 dilution in wash buffer) for 30 min at 4.0 °C. MAA-FITC (1:200 dilution in wash buffer) and LFA-FITC (1:50 dilution in wash buffer) staining was performed for 30 min at 4.0 °C. Cells were washed twice, then analyzed by flow cytometry.

Periodate-resorcinol determination of sialic acid concentration

Wt* or G2E* cells were incubated with the indicated substrate or with no substrate. Cells were grown to a density between 6.0×10^5 and 9.0×10^5 cells/ml over three days and the periodate-resorcinol assay was performed as described (28,31).

Synthesis of compound 1

Hydroxylamine hydrochloride (4.0 g, 0.057 mol) and sodium methoxide (3.0 g, 0.057 mol) were stirred in methanol for 30 min. The resulting white salts were removed by filtration. H₂O (30 ml) and GlcNAc (5.0 g, 0.022 mol) were added to the filtrate and the reaction was stirred for 18 h at 40 °C. The reaction was concentrated and filtered through a plug of silica, eluting with 5:1 CHCl₃:MeOH to yield the desired product (5.2 g, 100%). Compound **1** was further purified for enzymatic assays by recrystallization from acetonitrile and methanol, then characterized as a mixture of *E* and *Z* isomers. ¹H NMR (500 MHz, D₂O): δ 1.89 (3H, s), 1.89 (3H, s), 3.35 (1H, dd, *J* = 2.0, 8.5), 3.39 (1H, dd, *J* = 2.0, 8.5), 3.47 (2H, dd, *J* = 6.5, 12.0), 3.60 (2H, m), 3.68 (2H, *J* = 3.0, 12.0), 3.92 (1H, dd, *J* = 2.0, 7.5), 3.96 (1H, dd, *J* = 2.0, 7.5), 4.54 (1H, dd, *J* = 6.0, 7.5), 5.02 (1H, app t, *J* = 7.3), 6.64 (1H, d, *J* = 6.5), 7.32 (1H, d, *J* = 6.0). ¹³C NMR (125 MHz, D₂O): δ 20.9, 47.5, 52.0, 63.0, 69.5, 70.2, 71.1, 149.5, 150.0, 174.2. FAB-HRMS calcd. for (M+H⁺) 237.2305, found 237.1087.

Synthesis of compound 3

Acetic anhydride (5.0 ml, 0.055 mol) was added to a solution of **2** (1.0 g, 0.0045 mol) in pyridine (10 ml) and the reaction was stirred overnight at room temperature. The solution was concentrated, dissolved in CHCl₃ and washed with 1.0 M HCl, NaHCO₃ and saturated NaCl. The organic phase was dried over MgSO₄, filtered and concentrated to give the crude product (0.64 g, 33%). This material was purified for metabolic experiments by reversed-phase HPLC, eluting with a gradient of CH₃CN (10-60%) and H₂O. The HPLC-purified compound was dissolved in ethanol (5.0 mM stock solution) and filtered (0.25 micron sterile filter) prior to incubation with cells. ¹H NMR (300 MHz, MeOD): δ 1.98 (3H, s), 2.00 (3H, s), 2.02 (3H, s),

Role of GlcNAc 2-epimerase

2.04 (3H, s), 2.05 (3H, s), 2.09 (3H, s), 3.91 (1H, dd, $J = 6.6, 11.3$), 4.12 (2H, m), 4.29 (1H, dd, $J = 3.9, 12.2$), 4.51 (1H, m), 5.08 (1H, m), 5.38 (1H, m). ^{13}C NMR (125 MHz, MeOD): δ 19.1, 19.2, 19.2, 19.3, 21.1, 61.1, 62.4, 69.0, 69.0, 69.7, 169.9, 170.1, 170.2, 170.7, 170.8, 172.1. FAB-HRMS calcd. for $(\text{M}+\text{H}^+)$ 434.4071, found 434.1662.

Protein expression and purification

For bacterial expression, the human GlcNAc 2-epimerase gene was cloned into pET28b(+). The GlcNAc 2-epimerase gene was amplified by PCR using *Pfu* DNA polymerase, MgSO_4 (5.0 mM) and the following cycling conditions: 96 °C for 5.0 min, then 30 cycles of 96 °C for 45 s, 60 °C for 45 s, 72 °C for 90 s, then 72 °C for 5.0 min. Primer sequences were as follows: 5' primer: 5'-GGTGGTGGTCATATGATGGAGAAAGAGCGAGAGACTCTGCA GG-3', 3' primer: 5'-CCGCCGGAATTCTTAGGAGCGGACTCAGCCTTTATTCCGCGC-3'. The PCR product and pET28b(+) were digested with *Nde* I and *Eco*R I and ligated with T4 DNA ligase. A 24 nucleotide C-terminal deletion in the gene was discovered when the resulting vector, pSJL41392, was sequenced. At that point, pSJL41392 was digested with *Kpn* I and *Eco*R I to excise the incorrect 850 bp C-terminal fragment of the GlcNAc 2-epimerase gene. The vector pUKHRB6 was digested with *Kpn* I and *Eco*R I to obtain the correct C-terminal fragment. Upon ligation with T4 DNA ligase, the correct C-terminus of the GlcNAc 2-epimerase gene was installed. DNA sequencing of the resulting vector, pSJL737, confirmed this result.

The vector pSJL737 was transformed into the *E. coli* strain BL21(DE3) and expression of GlcNAc 2-epimerase was induced with 1.0 mM IPTG for 5.0 h at 37 °C. The cells were lysed by sonication at 4.0 °C (5 x 20 s at 5.0 min intervals, constant duty cycle, level 3 on a Branson Sonifier 450), centrifuged and the supernatant was purified with His-bind resin according to the manufacturer's instructions. The protein was eluted with 1.0 M imidazole and fractions containing protein were dialyzed against a storage buffer (8 L, 20 mM sodium phosphate (pH 7.0), 1.0 mM EDTA, 5.0% sucrose and 1.0% β -mercaptoethanol (20)) for 24 h at 4.0 °C. For NMR experiments, the protein solution was lyophilized once from H_2O and twice from D_2O , and

Role of GlcNAc 2-epimerase

concentrated 2.0-fold. For colorimetric assays, GlcNAc 2-epimerase was lyophilized once and concentrated 2.0-fold. The protein was stored at $-80\text{ }^{\circ}\text{C}$ and found to be stable for at least six months.

Colorimetric assay for GlcNAc 2-epimerase

The colorimetric assay to detect the epimerization of ManNAc by GlcNAc 2-epimerase was performed as described (32), except that the enzymatic reactions were monitored continuously on a Molecular Devices SpectraMax 190 spectrophotometer to acquire initial rates. Trend lines for inhibition by **1** and **2** were determined from non-linear regression analysis using the program GraFit 4.0 and the data were fit to a competitive inhibition model using the non-linear regression analysis program, SAS. Trend lines did not converge to fit a noncompetitive pattern for either compound. There was a small background rate that could be attributed to the side reaction of ManNAc with the coupling enzymes, as previously reported (32). In all assays this background signal was subtracted to establish the actual rate of the reaction. In addition, at the highest inhibitor concentrations and lowest substrate concentrations, there was a significant background signal that was attributed to reaction of the inhibitor directly with the coupling enzymes. This value was subtracted but likely contributes some error to the rates measured using these data points.

^1H NMR assay for GlcNAc 2-epimerase activity

^1H NMR assays of GlcNAc 2-epimerase activity on ManNAc analogs were performed on a Bruker DRX-500 MHz spectrometer equilibrated to $37\text{ }^{\circ}\text{C}$. D_2O (225 μL), 4x enzyme buffer (125 μL , 400 mM Tris buffer (pH 7.4), 40 mM MgCl_2 , 16 mM ATP, lyophilized twice from D_2O) and alanine (50 μL , 11.95 mg/ml in D_2O , internal standard) were added to the desired monosaccharide (0.073 mmol) to constitute the reaction mixture. GlcNAc 2-epimerase (100 μL , enzyme concentration varied between preparations but all rates were normalized to the rate of conversion of ManNAc for each preparation) was added immediately prior to acquisition of the first spectrum. Spectra were acquired over various lengths of time depending on the

monosaccharide (1.0-10 h). The enzyme-catalyzed rate of epimerization for each monosaccharide was measured by integration of the peaks corresponding to H-1 of both anomers of ManNAc (or the ManNAc analog) at various time points. Using Microsoft Excel, the rate of disappearance of ManNAc (or the ManNAc analog) was calculated relative to the internal standard (alanine) that remained unchanged throughout the course of the reaction.

RESULTS

Introduction of GlcNAc 2-epimerase into human cells

Analysis of mRNA from the human T cell lymphoma line Jurkat by RT-PCR showed no detectable message for GlcNAc 2-epimerase, suggesting that ManNAc is produced exclusively by UDP-GlcNAc 2-epimerase in these cells. Accordingly, the mRNA encoding UDP-GlcNAc 2-epimerase was observed by RT-PCR (data not shown).

To achieve stable expression of GlcNAc 2-epimerase in Jurkat cells, we used the two-step FlpIn system (Invitrogen). This approach to stable transfection is particularly useful with genes that do not produce a readily selectable phenotype, as is the case with GlcNAc 2-epimerase. First, clonal populations of potential host Jurkat cells were generated that contain a Zeocin resistance gene, flanked by Flp Recombination Target (FRT) sites (DNA sequences recognized by Flp recombinase), stably integrated into the genome. In order to determine which host cell line would lead to the desired levels of gene expression, we introduced a reporter protein (dsRed) into selected clonal populations and screened the resulting cells by flow cytometry. One host cell line was selected based on relatively high, homogeneous expression of dsRed; this host cell line was denoted “wt*.” We expected that the expression of GlcNAc 2-epimerase introduced by the same method into wt* cells would yield a similar expression pattern. Like the parent Jurkat cells, wt* cells had no detectable mRNA encoding GlcNAc 2-epimerase (Figure 2, lane 3).

Second, a plasmid (pSJLG2E/FRT) containing the GlcNAc 2-epimerase and Hygromycin resistance genes, flanked by FRT sites, was introduced into wt* cells along with a plasmid (pOG44) containing the gene for Flp recombinase. Flp recombinase-mediated DNA recombination and selection using Hygromycin yielded wt* cells with the GlcNAc 2-epimerase gene stably integrated into the genome (the resulting population was denoted G2E*). The expression of the mRNA encoding GlcNAc 2-epimerase in G2E* cells was confirmed by RT-PCR analysis (Figure 2, lane 4).

Effect of GlcNAc 2-epimerase on metabolic flux within the sialic acid pathway

We next investigated the effect of GlcNAc 2-epimerase expression on cell surface sialic acid content. G2E* and wt* cells were stained with the conjugated lectins *Maackia Amurensis II* (MAA-FITC), which recognizes α -2,3-linked sialic acid, *Limax flavus* (LFA-FITC) and *Tritrichomonas mobilensis* (TML-biotin, followed by FITC-avidin), which recognize sialic acid in a linkage-independent fashion, and analyzed by flow cytometry. In all cases, G2E* cells showed very little change in fluorescence compared with wt* cells (data not shown).

Cell surface sialylation does not necessarily reflect the level of free sialic acid within cells. For example, a buildup of sialic acid will not be detected if downstream enzymes, such as the sialyltransferases, are functioning at capacity. Previously, our laboratory has demonstrated that ManNAc analogs bearing chemically detectable probes can be used as tools to monitor the metabolic flux within the sialic acid pathway. For example, analogs of ManNAc that contain a ketone (ManLev, Figure 3A) (33) or an azide (ManNAz) (26) within the *N*-acyl group are converted by cells to the corresponding sialic acids, SiaLev and SiaNAz, respectively. When expressed on the cell surface, these modified sialic acids can be reacted with chemical probes and quantified by flow cytometry (Figure 3B). Typically, ketones are detected with biotin hydrazide followed by FITC-avidin (34), and azides are detected with phosphines conjugated to the FLAG peptide followed by an anti-FLAG antibody (35). Since the ManNAc analogs

compete with endogenous ManNAc, changes in the intracellular concentration of native sialic acid intermediates will affect unnatural sialic acid expression on the cell surface. Thus, unnatural sialic acid expression can serve as a reporter of cellular metabolic flux. We have previously exploited this phenomenon to study regulatory mechanisms of sialoside expression (28).

In order to observe the effect of GlcNAc 2-epimerase expression on metabolic flux within the sialic acid pathway, we incubated wt* and G2E* cells with peracetylated forms of ManLev (Ac₄ManLev, Figure 3A) and ManNAz (Ac₄ManNAz) and then analyzed them by flow cytometry. The peracetylated sugars permeate cell membranes more readily than the unacetylated sugars and can therefore be used at lower concentrations (25,36). The acetyl groups are removed by non-specific esterases in the cytosol, liberating the free sugars inside cells. As shown in Figure 4, G2E* cells produced less unnatural sialic acid on the cell surface than wt* cells when both were treated with either Ac₄ManLev (Figure 4A) or Ac₄ManNAz (Figure 4B). In the case of Ac₄ManLev, the difference in cell surface fluorescence was 5-fold, whereas in the case of Ac₄ManNAz this difference was 17-fold. Thus, the presence of the epimerase reduces unnatural sialoside expression and the effect is more dramatic with the substrate bearing the smaller *N*-acyl group.

We have previously found that the size of the *N*-acyl group on ManNAc derivatives can affect the efficiency of unnatural sialic acid biosynthesis in cells (37) and substrate activity with isolated enzymes *in vitro* (38). Accordingly, we postulated that GlcNAc 2-epimerase catalyzes the epimerization of ManNAz to the corresponding *gluco* analog more efficiently than ManLev. To address this experimentally, we developed an *in vitro* ¹H NMR assay to measure the relative rates of the GlcNAc 2-epimerase-catalyzed reaction with the two unnatural substrates. As shown in Table 1, the enzyme epimerizes ManNAz 345 times more rapidly than ManLev, and both substrates react more slowly than ManNAc.

The effect of GlcNAc 2-epimerase on intracellular free sialic acid concentrations

To investigate the effect of GlcNAc 2-epimerase on the flux of natural sialic acid biosynthesis, we analyzed free sialic acid content in wt* and G2E* cells. Levels of glycoconjugate-bound and total sialic acid can be measured using the periodate-resorcinol assay and the level of free sialic acid can be determined by subtracting the former from the latter (31). The level of free sialic acid in untreated Jurkat cells is close to the detection limit of the assay and is difficult to measure reproducibly. Nonetheless, G2E* cells appeared to have lower concentrations of free sialic acid than wt* cells (Figure 5).

More reliable measurements were obtained by the addition of ManNAc, which increases the amount of free sialic acid in the cell well above the limit of detection. When both cell lines were treated with 10 mM ManNAc, G2E* cells clearly produced less sialic acid than wt* cells (Figure 5). Thus, in the presence of excess ManNAc, GlcNAc 2-epimerase acts to lower free sialic acid levels, presumably by diverting ManNAc to GlcNAc. The Jurkat cell lines were also both incubated with 10 mM GlcNAc and analyzed for the effect on sialic acid content. The addition of GlcNAc did not measurably increase the level of sialic acid in G2E* cells above that in wt* cells (Figure 5), suggesting that intracellular ManNAc concentrations did not differ significantly between the two cell lines. To rule out the possibility that the different effects of ManNAc and GlcNAc on sialic acid production were due to differential uptake by the cells, we performed the same experiment with the peracetylated derivatives. These compounds should equally penetrate cell membranes by passive diffusion (36). The peracetylated compounds had the same relative effects on sialic acid content in wt* and G2E* cells as observed with free ManNAc and GlcNAc (data not shown).

Substrate-based inhibitor of GlcNAc 2-epimerase

The previous experiments establish that GlcNAc 2-epimerase expression correlates with a reduction in sialic acid biosynthesis. In order to confirm that this reduction was the direct result

of enzyme activity, we designed an inhibitor of GlcNAc 2-epimerase for use in cellular studies. A mechanism describing the interconversion of GlcNAc and ManNAc by GlcNAc 2-epimerase was recently proposed by Samuel and Tanner (Figure 6A) (21), but has not been addressed experimentally. The proposed reaction involves ring-opening to enable abstraction of H-2 and formation of an enediol-like intermediate, resembling reactions catalyzed by D-ribulose-5-phosphate-3-epimerase (21,39), triose phosphate isomerase (40) and phosphoglucose isomerase (41,42). Although analogs of the enediol intermediate have been shown to inhibit these related enzymes (43-45), we opted for more synthetically tractable mimetics based on the ring-opened form of GlcNAc. We synthesized compounds **1** and **2** (Figure 6B) and adapted a published enzyme-coupled colorimetric assay for GlcNAc 2-epimerase to measure their inhibitory activity. The assay detects the production of GlcNAc by enzymatic oxidation of the C-6 hydroxyl group and concomitant production of hydrogen peroxide, which is subsequently consumed in a chromogenic peroxidase reaction (32). For ease of analysis we modified the assay to monitor the reaction continuously.

The value of K_M obtained for ManNAc (4.3 mM) was close to the literature value (13.2 mM) obtained using the endpoint assay (46). We then measured the inhibition constants (K_I) of **1** and **2** to be 90 μ M and 109 μ M, respectively. By varying the concentrations of substrate and inhibitor, we obtained kinetic data consistent with a competitive inhibition mechanism for both **1** and **2**, indicating that both analogs compete with ManNAc for the active site (Figure 7). To make an inhibitor useful in cell culture (36), compound **2** was acetylated to form compound **3** (Figure 6B).

GlcNAc 2-epimerase inhibitor is active in cells

Compound **3** was used to confirm that GlcNAc 2-epimerase activity was responsible for the reduced conversion of Ac₄ManLev to SiaLev in G2E* cells compared to wt* cells. As shown in Figure 8, compound **3** reverses the effect of GlcNAc 2-epimerase in a dose-dependent

fashion, nearly restoring unnatural sialic acid biosynthesis to wt* levels at 200 μ M. Importantly, the production of SiaLev in wt* cells was not significantly affected by the addition of **3**.

Finally, we incubated wt* and G2E* cells with ManNAc in the presence and absence of compound **3** and analyzed free sialic acid levels using the periodate-resorcinol assay (Figure 9). Although the sialic acid level in G2E* cells was still lower than that in wt* cells, the differential was significantly reduced by the GlcNAc 2-epimerase inhibitor (100 μ M). Thus, the inhibitor reverses the low sialic acid phenotype characteristic of G2E* cells, confirming that the enzyme is directly responsible for that phenotype.

DISCUSSION

To investigate the effect of GlcNAc 2-epimerase on intracellular metabolic flux within the sialic acid pathway, we initially analyzed cell surface sialic acid expression. Sialic acid-binding lectins revealed little about the changes in sialic acid metabolism resulting from GlcNAc 2-epimerase expression in Jurkat cells. However, we were able to observe an effect on sialic acid biosynthesis by using unnatural metabolic substrates and by measurements of intracellular sialic acid levels.

G2E* cells, which express GlcNAc 2-epimerase, were unable to convert two unnatural ManNAc analogs (Ac₄ManLev and Ac₄ManNAz) to the corresponding sialosides (SiaLev and SiaNAz) at levels comparable to wt* cells. This observation is consistent with epimerization of the ManNAc analogs to the corresponding GlcNAc analogs, and consequently, diversion from the sialic acid pathway. GlcNAc derivatives that are produced in this fashion could be utilized in other metabolic pathways that do not contribute to cell surface fluorescence, or they may be dead-end biosynthetic intermediates. This model for the effect of GlcNAc 2-epimerase on sialic acid biosynthesis is summarized in Figure 10A.

Alternatively, it may be possible that G2E* cells produce higher levels of ManNAc than wt* cells due to epimerization of GlcNAc, a model summarized in Figure 10B. Indeed, ManLev

was previously used by our laboratory as a tool to select a Jurkat cell line containing mutations in the UDP-GlcNAc 2-epimerase gene that make the protein resistant to inhibition by CMP-sialic acid (28). Lacking that regulatory mechanism, these cells overproduced ManNAc, which suppressed unnatural sialic acid expression by direct competition with ManLev. The models shown in Figure 10 are not mutually exclusive; GlcNAc 2-epimerase may perform either of these functions depending on the relative availabilities of GlcNAc and ManNAc in the cell.

GlcNAc 2-epimerase is clearly capable of converting ManNAz and ManLev to their *gluco* counterparts *in vitro*. The superior efficiency of ManNAz epimerization *in vitro* is consistent with the dramatic effect of epimerase expression on SiaNAz biosynthesis in cells. Furthermore, intracellular sialic acid levels are reduced in cells expressing GlcNAc 2-epimerase, an effect that cannot be reversed by the addition of exogenous GlcNAc. Collectively, these data support the first model (Figure 10A) in which GlcNAc 2-epimerase converts ManNAc and its analogs to the respective *gluco* isomers. In the case of the second model (Figure 10B), epimerase expression would be expected to boost intracellular sialic acid levels in the presence of excess GlcNAc. Furthermore, the conversion of ManNAz to SiaNAz would be suppressed to a lesser extent than the conversion of ManLev to SiaLev, since ManNAz is a more capable competitor with ManNAc in the sialic acid pathway (30). The data presented show the opposite effects, arguing against the second model.

To confirm that GlcNAc 2-epimerase was the causative agent of the observed changes in sialic acid biosynthesis in G2E* cells, we designed a family of inhibitors (compounds **1-3**) based on a proposed chemical mechanism of the enzyme (21) (Figure 6). The K_i values of **1** and **2** (90 and 109 μ M, respectively) were approximately 40-fold lower than the measured K_M value for ManNAc (4.3 mM) and 200-fold lower than the reported K_M value for GlcNAc (21.3 mM) (20). Since the inhibitors were designed to mimic the ring-opened form of GlcNAc, this lends support to the proposed mechanism in Figure 6A. The hydrophilicity of compounds **1** and **2** would likely

frustrate their activity in cell culture experiments. However, compound **3**, a peracetylated analog of **2**, demonstrated inhibitory activity in cells at micromolar concentration.

Introduction of compound **3** into G2E* cells in the presence of Ac₄ManLev resulted in a reversal of the phenotype attributed to GlcNAc 2-epimerase, indicating that the action of the enzyme was indeed responsible for the low cell surface expression of unnatural sialic acids (Figure 8). Additionally, unnatural sialic acid expression in wt* cells showed essentially no change when incubated with compound **3**, indicating that the inhibitor does not cross-react with other proteins in the cell that affect sialic acid biosynthesis. The low intracellular sialic acid level maintained by G2E* cells was increased by compound **3**, suggesting again that the inhibitor can reverse the phenotype associated with GlcNAc 2-epimerase expression.

It is possible that the primary function of GlcNAc 2-epimerase is to divert metabolic flux from sialic acid biosynthesis into other pathways reliant on GlcNAc or UDP-GlcNAc. Numerous glycoproteins and proteoglycans include GlcNAc as a component, and several cytosolic and nuclear proteins are modified with β -O-GlcNAc in a possible regulatory fashion (47,48). Increases in cellular GlcNAc may affect the flux in these pathways. Alternatively, phosphorylation of GlcNAc followed by deacetylation of GlcNAc 6-phosphate to glucosamine 6-phosphate generates a substrate for glycolysis (49). It is possible that GlcNAc 2-epimerase serves to increase glycolytic flux at the expense of protein glycosylation.

We conclude that GlcNAc 2-epimerase catalyzes the conversion of ManNAc (and ManNAc analogs) to GlcNAc (and GlcNAc analogs) in human cells, but the reverse process is unobservable, even in the presence of added GlcNAc. Furthermore, analogs of the ring-opened form of GlcNAc are effective inhibitors of GlcNAc 2-epimerase *in vitro*, lending support to a proposed chemical mechanism. One of these inhibitors reversed the sialic acid reduction induced by GlcNAc 2-epimerase, confirming that the phenotype observed was directly attributable to activity of the enzyme and demonstrating the utility of the inhibitor in human cells. Based on the results presented here, we propose that GlcNAc 2-epimerase is not an

alternate route to ManNAc production in cells. Rather, the enzyme diverts metabolic flux away from sialic acid biosynthesis, performing a function distinct from that of UDP-GlcNAc 2-epimerase.

ACKNOWLEDGMENTS

We thank Hector Nolla for assistance with flow cytometry. This research was supported by grants to C.R.B. from the National Institutes of Health (GM58867) and the Director, Office of Science, Office of Basic Energy Sciences, Division of Materials Sciences and Engineering and the Office of Energy Biosciences of the U.S. Department of Energy under Contract No. DE-AC03-76SF00098.

REFERENCES

1. Brockhausen, I. (1999) *Biochim. Biophys. Acta* **1473**, 67-95.
2. Blackhall, F. H., Merry, C. L., Davies, E. J., and Jayson, G. C. (2001) *Br. J. Cancer* **85**, 1094-8.
3. Dwek, R. A. (1996) *Chem. Rev.* **96**, 683-720.
4. Varki, A. (1993) *Glycobiology* **3**, 97-130.
5. Vestweber, D., and Blanks, J. E. (1999) *Physiol. Rev.* **79**, 181-213.
6. Crocker, P. R., and Varki, A. (2001) *Immunol.* **103**, 137-145.
7. Keppler, O. T., Horstkorte, R., Pawlita, M., Schmidt, C., and Reutter, W. (2001) *Glycobiology* **11**, 11R-18R.
8. Stäsche, R., Hinderlich, S., Weise, C., Effertz, K., Lucka, L., Moormann, P., and Reutter, W. (1997) *J. Biol. Chem.* **272**, 24319-24.

9. Lucka, L., Krause, M., Danker, K., Reutter, W., and Horstkorte, R. (1999) *FEBS Lett.* **454**, 341-4.
10. Lawrence, S. M., Huddleston, K. A., Pitts, L. R., Nguyen, N., Lee, Y. C., Vann, W. F., Coleman, T. A., and Betenbaugh, M. J. (2000) *J. Biol. Chem.* **275**, 17869-77.
11. Münster, A. K., Eckhardt, M., Potvin, B., Mühlenhoff, M., Stanley, P., and Gerardy-Schahn, R. (1998) *Proc. Natl. Acad. Sci. U.S.A.* **95**, 9140-5.
12. Lawrence, S. M., Huddleston, K. A., Tomiya, N., Nguyen, N., Lee, Y. C., Vann, W. F., Coleman, T. A., and Betenbaugh, M. J. (2001) *Glycoconj. J.* **18**, 205-13.
13. Troy, F. A., 2nd. (1992) *Glycobiology* **2**, 5-23.
14. Kikuchi, K., and Tsuiki, S. (1973) *Biochim. Biophys. Acta* **327**, 193-206.
15. Keppler, O. T., Hinderlich, S., Langner, J., Schwartz-Albiez, R., Reutter, W., and Pawlita, M. (1999) *Science* **284**, 1372-1376.
16. Schwarzkopf, M., Knobeloch, K. P., Rohde, E., Hinderlich, S., Wiechens, N., Lucka, L., Horak, I., Reutter, W., and Horstkorte, R. (2002) *Proc. Natl. Acad. Sci. U.S.A.* **99**, 5267-70.
17. Sommar, K. M., and Ellis, D. B. (1972) *Biochim. Biophys. Acta* **268**, 581-9.
18. Ghosh, S., and Roseman, S. (1965) *J. Biol. Chem.* **240**, 1531-1536.
19. Maru, I., Ohta, Y., Murata, K., and Tsukada, Y. (1996) *J. Biol. Chem.* **271**, 16294-9.
20. Takahashi, S., Takahashi, K., Kaneko, T., Ogasawara, H., Shindo, S., and Kobayashi, M. (1999) *J. Biochem. (Tokyo)* **125**, 348-53.
21. Samuel, J., and Tanner, M. E. (2002) *Nat. Prod. Rep.* **19**, 261-277.
22. Takahashi, S., Inoue, H., and Miyake, Y. (1992) *J. Biol. Chem.* **267**, 13007-13.
23. Schmitz, C., Gotthardt, M., Hinderlich, S., Lehesté, J. R., Gross, V., Vorum, H., Christensen, E. I., Luft, F. C., Takahashi, S., and Willnow, T. E. (2000) *J. Biol. Chem.* **275**, 15357-62.
24. Horstkorte, R., Nöhring, S., Wiechens, N., Schwarzkopf, M., Danker, K., Reutter, W., and Lucka, L. (1999) *Eur. J. Biochem.* **260**, 923-7.

25. Jacobs, C. L., Yarema, K. Y., Mahal, L. K., Nauman, D. A., Charters, N. W., and Bertozzi, C. R. (2000) *Meth. Enzymol.* **327**, 260-275.
26. Saxon, E., and Bertozzi, C. R. (2000) *Science* **287**, 2007-10.
27. Aspinall, G. O., Gharia, M. M., and Wong, C. O. (1980) *Carb. Res.* **78**, 275-283.
28. Yarema, K. J., Goon, S., and Bertozzi, C. R. (2001) *Nat. Biotechnol.* **19**, 553-8.
29. Nauman, D. A., and Bertozzi, C. R. (2001) *Biochim. Biophys. Acta* **1568**, 147-154.
30. Saxon, E., Luchansky, S. J., Hang, H. C., Yu, C., Lee, S. C., and Bertozzi, C. R. (2002) *J. Am. Chem. Soc.* **124**, 14893-14902.
31. Jourdian, G. W., Dean, L., and Roseman, S. (1971) *J. Biol. Chem.* **246**, 430-435.
32. Takahashi, S., Kumagai, M., Shindo, S., Saito, K., and Kawamura, Y. (2000) *J. Biochem. (Tokyo)* **128**, 951-6.
33. Mahal, L. K., Yarema, K. J., and Bertozzi, C. R. (1997) *Science* **276**, 1125-8.
34. Yarema, K. J., Mahal, L. K., Bruehl, R. E., Rodriguez, E. C., and Bertozzi, C. R. (1998) *J. Biol. Chem.* **273**, 31168-79.
35. Kiick, K. L., Saxon, E., Tirrell, D. A., and Bertozzi, C. R. (2002) *Proc. Natl. Acad. Sci. U.S.A.* **99**, 19-24.
36. Sarkar, A. K., Fritz, T. A., Taylor, W. H., and Esko, J. D. (1995) *Proc. Natl. Acad. Sci. U.S.A.* **92**, 3323-7.
37. Jacobs, C. L., Goon, S., Yarema, K. J., Hinderlich, S., Hang, H. C., Chai, D. H., and Bertozzi, C. R. (2001) *Biochemistry* **40**, 12864-74.
38. Jacobs, C. L., Hinderlich, S., Goon, S., Viswanathan, K., Weedin, J. W., Blume, A., Betenbaugh, M. J., Reutter, W., and Bertozzi, C. R. (2002), submitted.
39. Adams, E. (1976) *Adv. Enzymol. Relat. Areas Mol. Biol.* **44**, 69-138.
40. Rieser, S. V., and Rose, I. A. (1959) *J. Biol. Chem.* **234**, 1007-1010.
41. Rose, I. A., and O'Connell, E. L. (1961) *J. Biol. Chem.* **236**, 3086-3092.

42. Schray, K. J., Benkovic, S. J., Benkovic, P. A., and Rose, I. A. (1973) *J. Biol. Chem.* **248**, 2219-24.
43. Hardre, R., Bonnette, C., Salmon, L., and Gaudemer, A. (1998) *Bioorg. Med. Chem. Lett.* **8**, 3435-8.
44. Chirgwin, J. M., and Noltmann, E. A. (1975) *J. Biol. Chem.* **250**, 7272-6.
45. Collins, K. D. (1974) *J. Biol. Chem.* **249**, 136-42.
46. Takahashi, S., Hori, K., Takahashi, K., Ogasawara, H., Tomatsu, M., and Saito, K. (2001) *J. Biochem. (Tokyo)* **130**, 815-21.
47. Torres, C. R., and Hart, G. W. (1984) *J. Biol. Chem.* **259**, 3308-17.
48. Wells, L., Vosseller, K., and Hart, G. W. (2001) *Science* **291**, 2376-8.
49. Stamford, N. P. J. (ed) (2001) *Biosynthesis and Degradation* Vol. 2. Glycoscience. Edited by Fraser-Reid, B., Tatsuta, K., and Thiem, J. 3 vols., Springer-Verlag, New York.

¹ The abbreviations used are: ManNAc, *N*-acetylmannosamine; IPTG, isopropylthio- β -galactoside; Siglecs, sialic-acid binding immunoglobulin superfamily lectins; sLe^x, sialyl Lewis x; GlcNAc, *N*-acetylglucosamine; FITC, fluorescein isothiocyanate; MAA, *Maackia Amurensis* II; LFA, *Limax flavus*; TML, *Tritrichomonas mobilensis*; Ac₄ManLev, peracetylated *N*-levulinoylmannosamine; ManLev, *N*-levulinoylmannosamine; Ac₄ManNAz, peracetylated *N*-azidoacetylmannosamine; ManNAz, *N*-azidoacetylmannosamine; wt* cells, Jurkat cells containing an FRT site; G2E* cells, Jurkat cells containing GlcNAc 2-epimerase; FRT, Flp Recombinase Target; FCS, fetal calf serum; FLAG peptide, NH₂-DYKDDDDK-COOH; SiaLev, *N*-levulinoylneuraminic acid; SiaNAz, *N*-azidoacetylneuraminic acid.

Table 1: Relative rates of epimerization of ManNAc and ManNAc analogs by GlcNAc 2-epimerase determined by ^1H NMR. The assays were performed as described in Experimental Procedures. The standard deviation represents the error of three replicate experiments.

Figure 1: Sialic acid biosynthesis. *N*-Acetylmannosamine (ManNAc) is synthesized from UDP-*N*-acetylglucosamine (UDP-GlcNAc) by UDP-GlcNAc 2-epimerase but the role of GlcNAc 2-epimerase is unclear. ManNAc or a ManNAc analog is phosphorylated by ManNAc 6-kinase to yield ManNAc 6-phosphate (ManNAc 6-P). ManNAc 6-P is subsequently condensed with phosphoenolpyruvate (PEP) to yield sialic acid 9-phosphate (sialic acid 9-P) in a reaction catalyzed by sialic acid 9-P synthase. Dephosphorylation of sialic acid 9-P by an unknown phosphatase and transport to the nucleus enables CMP-sialic acid synthetase to produce CMP-sialic acid. Following transport into the Golgi compartment, CMP-sialic acid is utilized by the sialyltransferases that append the sialic acid to glycoconjugates ultimately destined for the cell surface or secretion.

Figure 2: Amplification of mRNA isolated from wt* and G2E* cells by RT-PCR. Lane 1: molecular weight marker. Lane 2: control RNA provided with the SuperScript First-Strand Synthesis RT-PCR kit (expected length: 500 bp). Lane 3: PCR amplification of cDNA from wt* cells with primers to human GlcNAc 2-epimerase (expected length: 809 bp). Lane 4: PCR amplification of cDNA from G2E* cells with primers to human GlcNAc 2-epimerase. Lane 5: PCR amplification of cDNA from wt* cells with primers to mouse β -actin (expected length: 540 bp). Lane 6: PCR amplification of cDNA from G2E* cells with primers to mouse β -actin.

Figure 3: Unnatural sialic acid biosynthesis as a tool for measuring metabolic flux. A. Unnatural monosaccharides that mimic ManNAc are taken up by cells as the peracetylated derivatives, then deacetylated by cytosolic esterases to yield the free ManNAc derivatives.



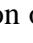

These substrates are converted into sialic acid derivatives by the enzymes in the sialic acid pathway and delivered to the cell surface. B. Schematic representation of the detection of unnatural ManNAc derivatives on the cell surface with chemical probes. In step 1, cells convert one of the unnatural analogs () shown in A to the corresponding unnatural cell surface sialoside (). The chemical handle associated with the unnatural sugar is derivatized in step 2 with a hydrazide or phosphine reagent linked to a detectable marker such as biotin or the FLAG peptide (). In step 3, detection of the conjugate is achieved with a fluorescent probe such as FITC-avidin or a FITC-conjugated anti-FLAG antibody (). The labeled cells are analyzed by flow cytometry as described in Experimental Procedures.

Figure 4: Flow cytometry plots representing wt* (black) and G2E* (gray) cells exposed to unnatural ManNAc analogs. Wt* and G2E* cells were incubated with 20 μ M Ac₄ManLev (A) or 20 μ M Ac₄ManNAz (B) and analyzed by flow cytometry as described in Figure 3 and Experimental Procedures. The background fluorescence of G2E* cells (white) is similar to that of wt* cells (data not shown). The plots shown are representative of data collected from three replicate experiments.

Figure 5: Free sialic acid levels in wt* (solid bars) and G2E* (striped bars) cells determined using the periodate-resorcinol assay. Untreated cells and cells incubated with 10 mM ManNAc or 10 mM GlcNAc were assayed for glycoconjugate-bound and total sialic acid as described in Experimental Procedures. Free sialic acid levels were calculated from these values. The error bars represent the standard deviation of three replicate experiments.

Figure 6: Proposed chemical mechanism and substrate-based inhibitors of GlcNAc 2-epimerase. A. The proposed mechanism of GlcNAc 2-epimerase involves ring-opening of the sugar to enable abstraction of H-2 and formation of an enediol-like intermediate. The intermediate can be

reprotonated from either face to yield the epimer or the starting monosaccharide. B. Compounds that inhibit GlcNAc 2-epimerase *in vitro* (**1** and **2**) or in cell culture (**3**).

Figure 7: Lineweaver-Burk analysis of inhibitors **1** and **2** with GlcNAc 2-epimerase using ManNAc as a substrate. A. Compound **1** exhibits a K_i of $90 \pm 4 \mu\text{M}$. Concentrations of inhibitor: $\square = 0 \mu\text{M}$, $\circ = 125 \mu\text{M}$, $\blacktriangle = 375 \mu\text{M}$, $\bullet = 1 \text{ mM}$. B. Compound **2** exhibits a K_i of $109 \pm 8 \mu\text{M}$. Concentrations of inhibitor: $\square = 0 \mu\text{M}$, $\circ = 100 \mu\text{M}$, $\blacktriangle = 250 \mu\text{M}$, $\bullet = 1 \text{ mM}$. Assays were performed in triplicate for each concentration of substrate and calculated K_i values were obtained from the nonlinear regression analysis program, SAS.

Figure 8: The inhibitory effect of GlcNAc 2-epimerase on SiaLev production can be reversed with compound **3**. Wt* (solid bars) and G2E* (striped bars) cells were incubated with $20 \mu\text{M}$ Ac₄ManLev and various concentrations of **3**. Flow cytometry was performed as described in Figure 3 and Experimental Procedures. Error bars represent the standard deviation of three replicate experiments.

Figure 9: Compound **3** reverses the effect of GlcNAc 2-epimerase on sialic acid production in G2E* cells. Glycoconjugate-bound and total sialic acid levels were measured in untreated wt* and G2E* cells and in cells incubated with 10 mM ManNAc in the presence and absence of compound **3** ($100 \mu\text{M}$). Free sialic acid levels were calculated from these values. The error bars represent the standard deviation of three replicate experiments. The free sialic acid levels in ManNAc-supplemented G2E* cells with and without compound **3** are significantly different as determined by a value of $P < 0.02$ (Two-Tailed t Test).

Figure 10: Possible mechanisms for reduced sialic acid biosynthetic flux in G2E* compared to wt* cells. A. GlcNAc 2-epimerase converts ManNAc (and ManNAc analogs) into GlcNAc (and

GlcNAc analogs), decreasing the production of natural and unnatural sialic acids. B. GlcNAc 2-epimerase increases ManNAc production which competes with unnatural ManNAc in the sialic acid biosynthetic pathway.

Table 1

Compound	Relative rates	std. dev.
ManNAc	909	27.0
ManNAz	345	90.0
ManLev	1	0.1

Figure 1

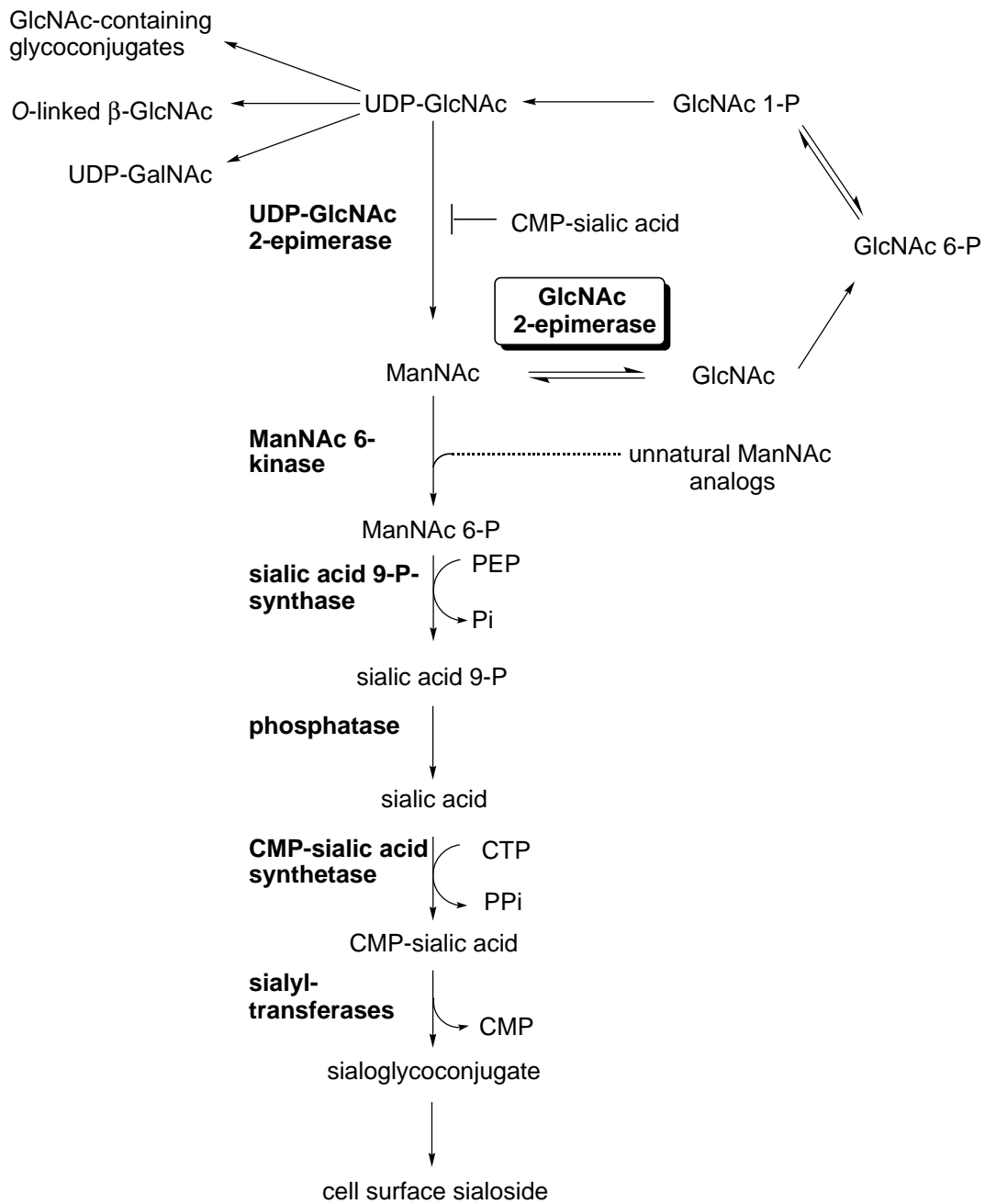


Figure 2

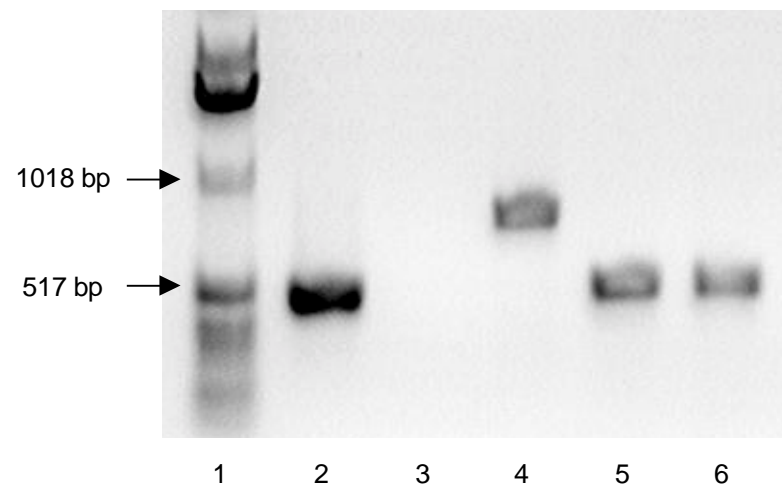
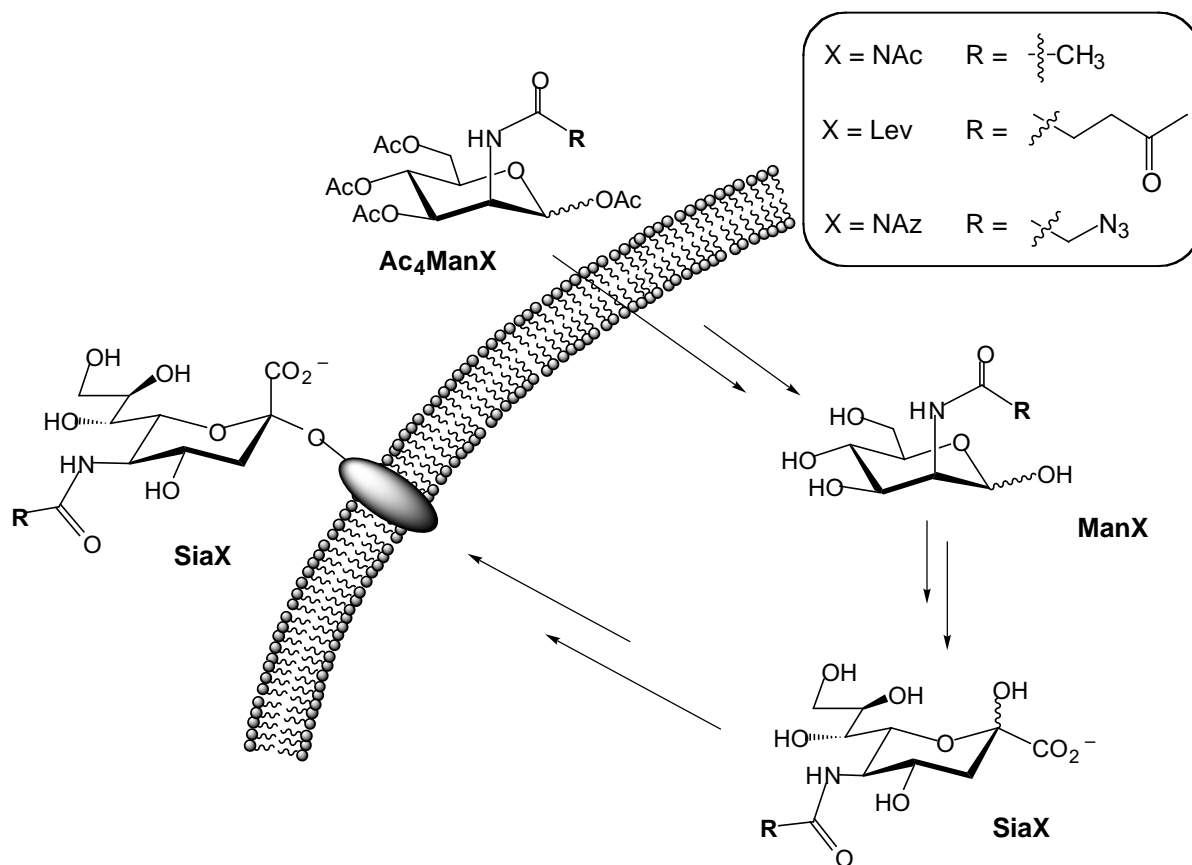


Figure 3

A.



B.

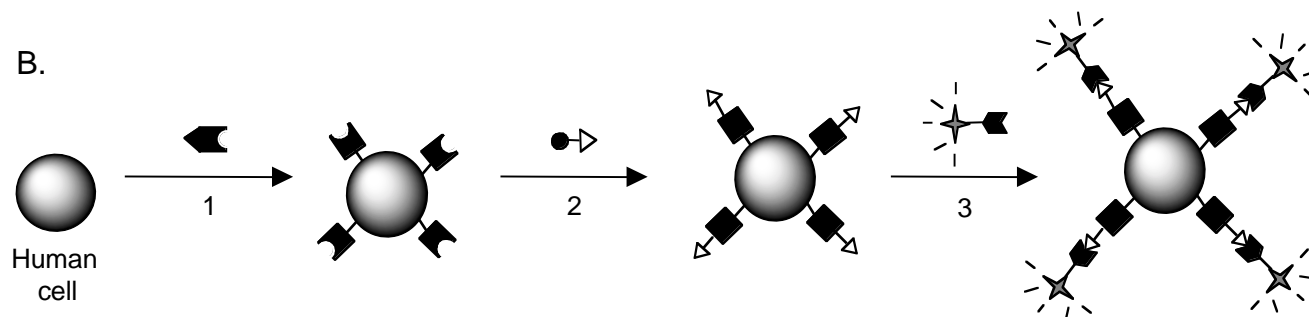


Figure 4

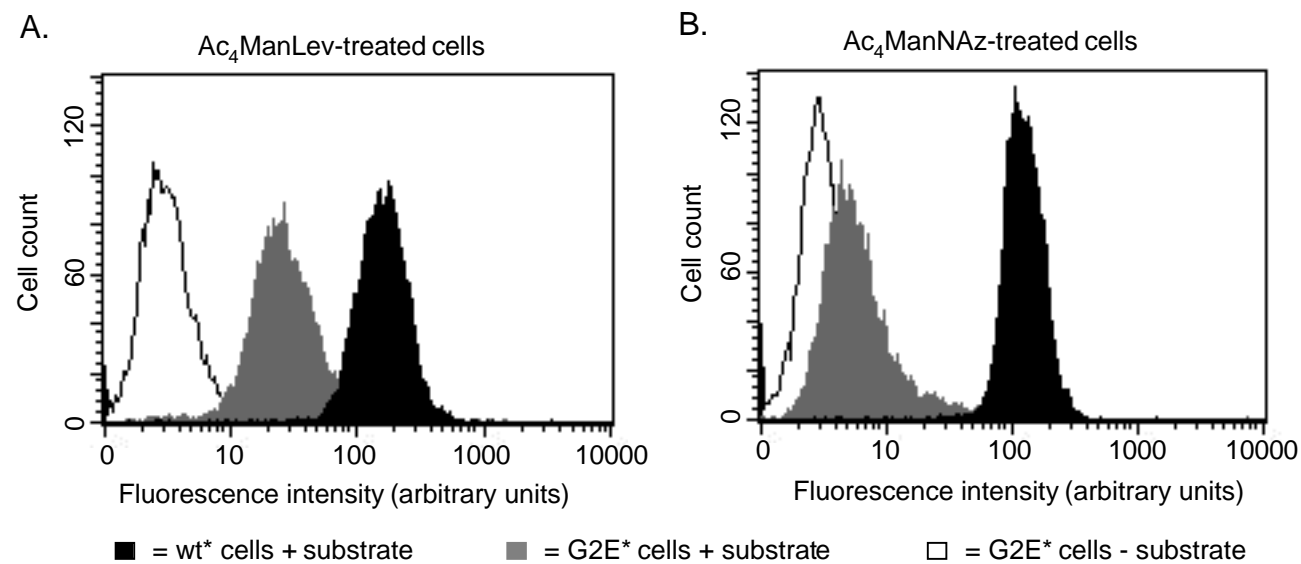


Figure 5

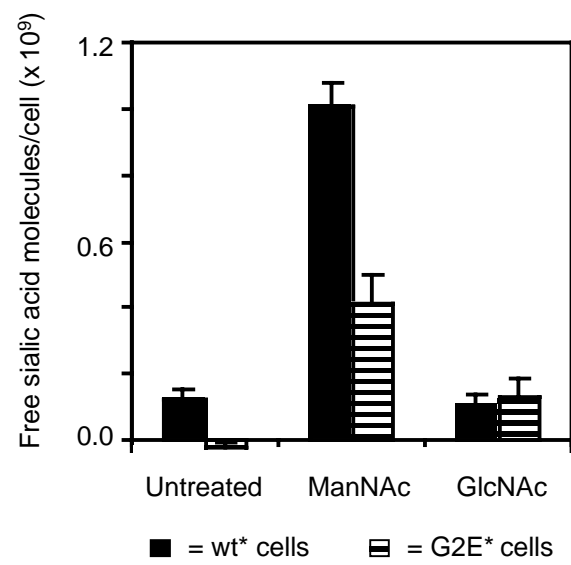
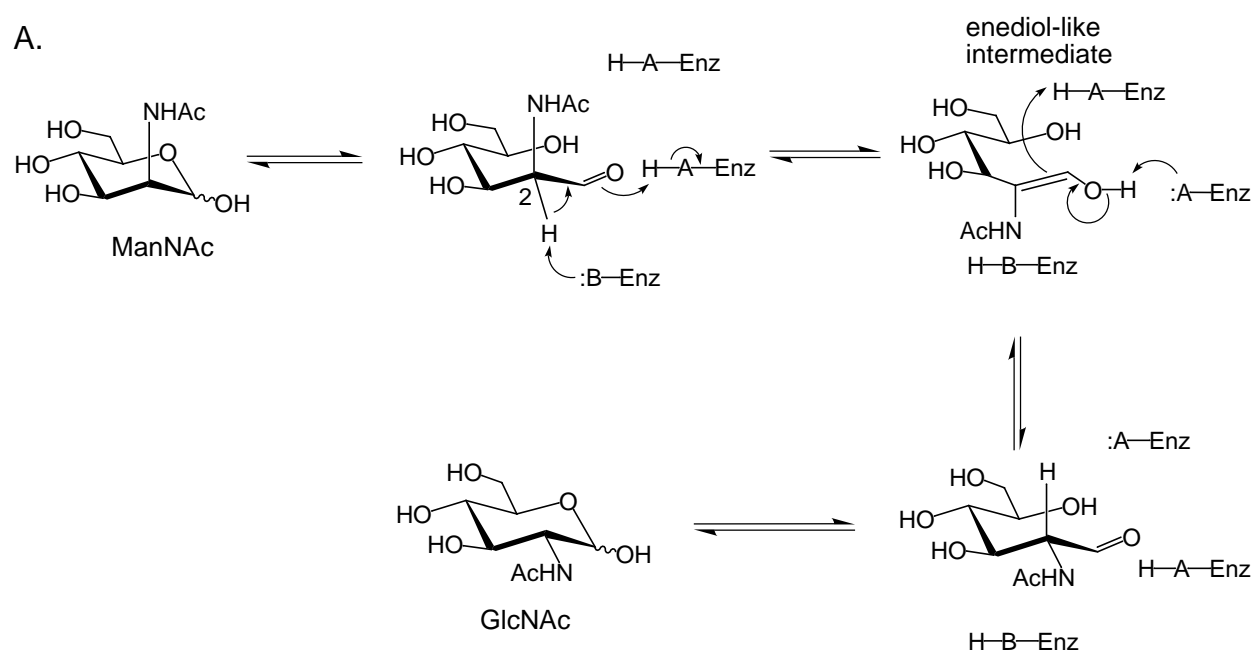


Figure 6

A.



B.

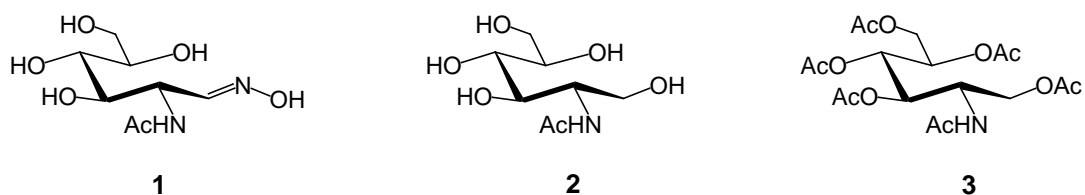


Figure 7

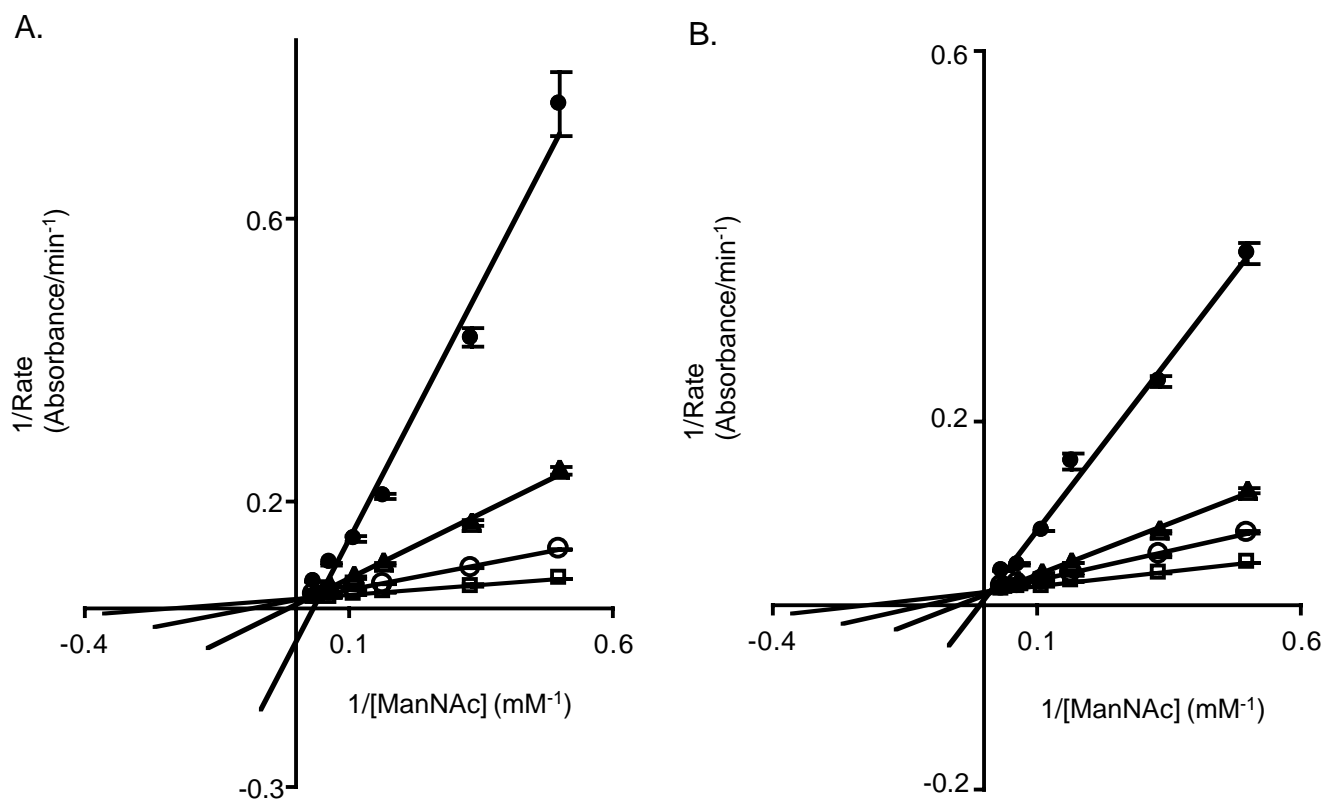


Figure 8

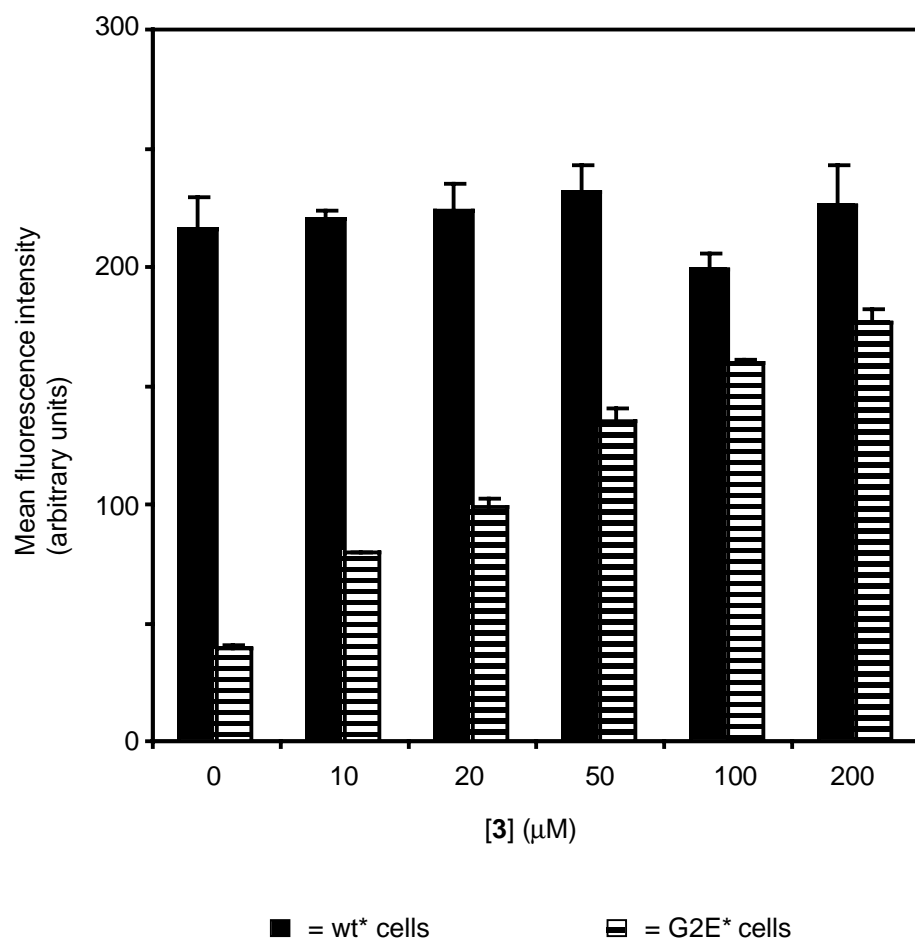


Figure 9

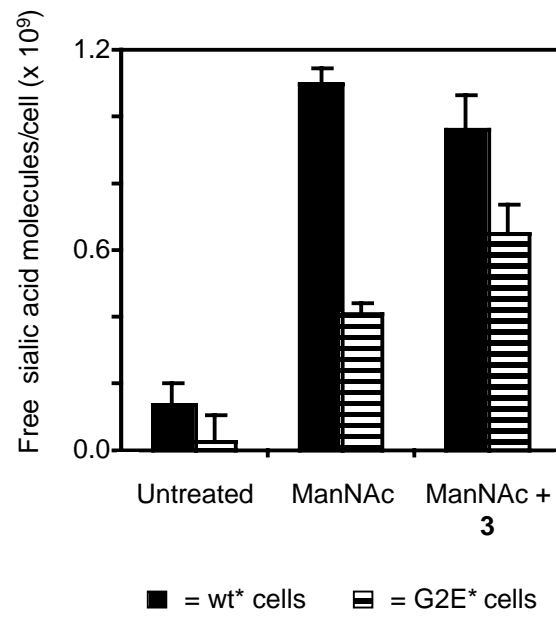
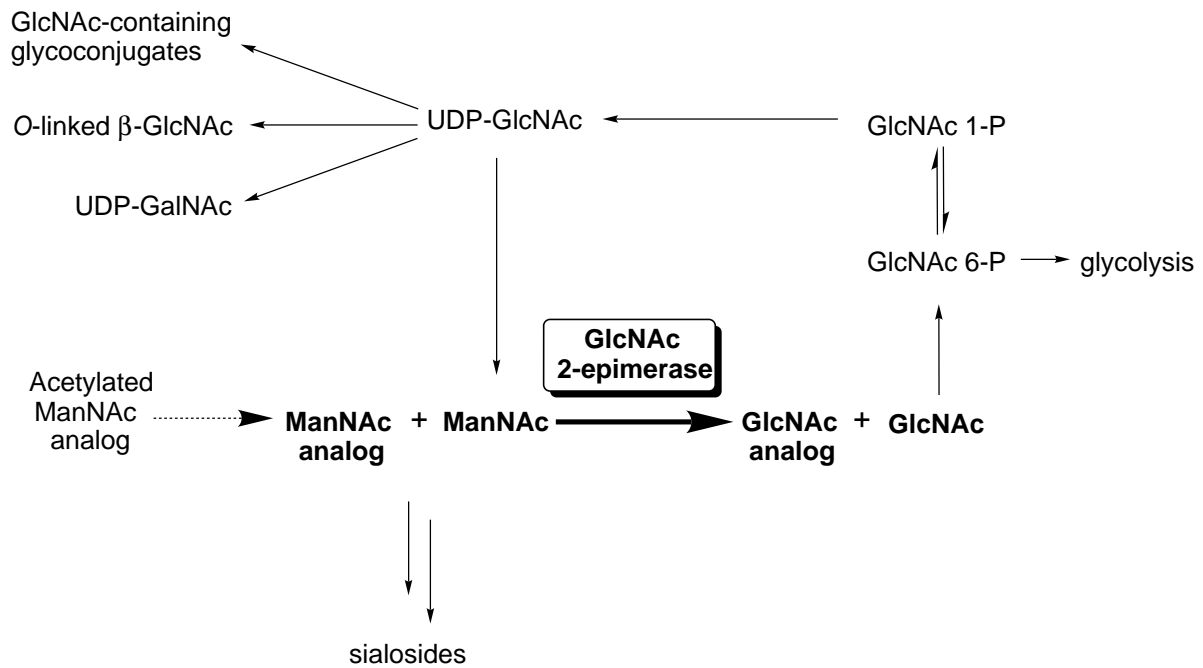


Figure 10

A.



B.

